AIP | Physics of Plasmas

Magnetic islands and singular currents at rational surfaces in three-dimensional magnetohydrodynamic equilibria

J. Loizu, S. Hudson, A. Bhattacharjee, and P. Helander

Citation: Physics of Plasmas (1994-present) **22**, 022501 (2015); doi: 10.1063/1.4906888
View online: http://dx.doi.org/10.1063/1.4906888
View Table of Contents: http://scitation.aip.org/content/aip/journal/pop/22/2?ver=pdfcov
Published by the AIP Publishing

Magnetic islands and singular currents at rational surfaces in three-dimensional magnetohydrodynamic equilibria

J. Loizu,[1,2,a)] S. Hudson,[2] A. Bhattacharjee,[2] and P. Helander[1]
[1]*Max-Planck-Institut für Plasmaphysik, D-17491 Greifswald, Germany*
[2]*Princeton Plasma Physics Laboratory, P.O. Box 451, Princeton New Jersey 08543, USA*

(Received 23 October 2014; accepted 9 January 2015; published online 2 February 2015)

Using the recently developed *multiregion, relaxed MHD* (MRxMHD) theory, which bridges the gap between Taylor's relaxation theory and ideal MHD, we provide a thorough analytical and numerical proof of the formation of singular currents at rational surfaces in non-axisymmetric ideal MHD equilibria. These include the force-free singular current density represented by a Dirac δ-function, which presumably prevents the formation of islands, and the Pfirsch-Schlüter $1/x$ singular current, which arises as a result of finite pressure gradient. An analytical model based on linearized MRxMHD is derived that can accurately (1) describe the formation of magnetic islands at resonant rational surfaces, (2) retrieve the ideal MHD limit where magnetic islands are shielded, and (3) compute the subsequent formation of singular currents. The analytical results are benchmarked against numerical simulations carried out with a fully nonlinear implementation of MRxMHD. © *2015 AIP Publishing LLC*. [http://dx.doi.org/10.1063/1.4906888]

I. INTRODUCTION

Ideal MHD with nested flux surfaces predicts the existence of singular current densities forming at rational surfaces in three-dimensional equilibria.[1–5] These current singularities consist of a Pfirsch-Schlüter component, which arises as a result of finite pressure gradient, and a δ-function current density, which presumably prevents the formation of islands that would otherwise develop in a non-ideal plasma. The singularities arise from requiring the conservation of charge, $\nabla \cdot \mathbf{j} = 0$, which gives rise to a magnetic differential equation for the parallel current, namely, $\mathbf{B} \cdot \nabla u = -\nabla \cdot \mathbf{j}_\perp$, where $\mathbf{j} \equiv u\mathbf{B} + \mathbf{j}_\perp$. Magnetic differential equations are densely singular.[6] Their singular nature is exposed as follows. First, straight-field-line coordinates may be constructed on each flux surface, giving $\sqrt{g}\mathbf{B} \cdot \nabla = \iota\partial_\theta + \partial_\zeta$. Here, $\sqrt{g}$ is the Jacobian of the coordinates, ι is the rotational transform on a given flux surface, and θ and ζ are the poloidal and toroidal straight-field-line angles, respectively. Then, by using a Fourier representation, $u = \sum_{mn} u_{mn} \exp[i(m\theta - n\zeta)]$, the magnetic differential equation implies

$$u_{mn}(x) = h_{mn}(x)/x + \Delta_{mn}\delta(x), \tag{1}$$

where $x = \iota m - n$, $h_{mn} = i(\sqrt{g}\nabla \cdot \mathbf{j}_\perp)_{mn}$, and Δ_{mn} is an arbitrary constant. The first term on the right-hand-side of Eq. (1) is the Pfirsch-Schlüter component of the parallel current and presents a $1/x$ singularity around rational surfaces. Its magnitude is proportional to the pressure gradient by virtue of the force-balance equation $\mathbf{j} \times \mathbf{B} = \nabla p$, which gives $\mathbf{j}_\perp = \mathbf{B} \times \nabla p/B^2$. The second term on the right-hand-side of Eq. (1) is a parallel δ-current density at the rational surfaces. Its magnitude, Δ_{mn}, remains undetermined here.

Since rational numbers are dense in real space, the singular currents implied by Eq. (1) are expected to be densely packed within the plasma volume, unless ι is irrational *and* constant across flux surfaces.

While analytical formulations have been developed to describe such currents in simplified geometries,[7,8] and the δ-currents have been computed using either ideal MHD initial value codes[9] or linearized, perturbed ideal equilibrium codes,[10,11] a numerical proof of their existence using nonlinear MHD equilibrium codes has been hampered by the assumption of smooth functions made in conventional MHD equilibrium models such as VMEC.[12] In particular, to our knowledge, no numerical model has been shown to compute the $1/x$ pressure-driven singular currents.

Recently, a theory based on a generalized energy principle, referred to as *multiregion, relaxed MHD* (MRxMHD), was developed and incorporates the possibility of non-smooth solutions to the MHD equilibrium problem and bridges the gap between Taylor's relaxation theory[13] and ideal MHD. In this paper, we develop an analytical model based on linearized MRxMHD theory and compare the predictions of this model to those of a fully nonlinear numerical implementation of MRxMHD.

The linearized model can accurately (i) describe the formation of magnetic islands at resonant rational surfaces, (ii) retrieve the ideal MHD limit in which magnetic islands are shielded, and (iii) compute the subsequent formation of both δ-currents and pressure-driven $1/x$ currents. The model is restricted to slab, linearly perturbed equilibrium solutions. However, to our knowledge, this is the first model that can achieve points (i)–(iii) at the same time.

We provide a numerical proof of the formation of singular currents in non-axisymmetric ideal MHD equilibria by leveraging a fully nonlinear numerical implementation of the MRxMHD model. For each numerical result, we perform careful convergence studies and analytical benchmarks.

In Sec. II, we summarize the main elements of the MRxMHD theory. The analytical model based on the

a)Electronic mail: joaquim.loizu@ipp.mpg.de

linearized MRxMHD theory is derived in Sec. III, showing that both magnetic islands and singular currents can be captured by the same model. In Sec. IV, we use a fully nonlinear implementation of the MRxMHD theory to benchmark the linear results. A conclusion and outlook follow in Sec. V.

II. MRxMHD THEORY

The classical MHD energy functional[14] is

$$W = \int_{V_p} \left(\frac{p}{\gamma - 1} + \frac{B^2}{2\mu_0} \right) dV, \tag{2}$$

where V_p is the plasma volume and γ is the adiabatic index. Ideal MHD equilibria are found by extremizing W subject to certain constraints. First, because the fluid is assumed to be perfectly conducting, the magnetic field is frozen into the plasma and cannot change its topology. For a given plasma displacement $\boldsymbol{\xi}$, Faraday's law and ideal Ohm's law restrict the possible variations of $\mathbf{B}$ to the form $\delta\mathbf{B} = \nabla \times (\boldsymbol{\xi} \times \mathbf{B})$. This is a continuous topological constraint that is equivalent to the conservation of magnetic helicity[13,15]

$$K = \int_V \mathbf{A} \cdot \mathbf{B}\, dV, \tag{3}$$

for any volume V bound by field lines in the plasma. Here, $\mathbf{A}$ is the vector potential such that $\mathbf{B} = \nabla \times \mathbf{A}$. The magnetic helicity can be related to the Gauss linking number and thus can be interpreted as a measure of how intertwisted are field lines.[16] Second, the continuity equation, $\partial_t \rho + \nabla \cdot (\rho \mathbf{v}) = 0$, and the equation of state, $d_t(p/\rho^\gamma) = 0$, constrain the possible variations of pressure. Here, p is the plasma pressure, ρ is the plasma density, $\mathbf{v}$ is the mean plasma velocity, and $d_t = \partial_t + \mathbf{v} \cdot \nabla$. These equations translate into the constraint $\delta p = (\gamma - 1)\boldsymbol{\xi} \cdot \nabla p - \gamma \nabla \cdot (p\boldsymbol{\xi})$. The first variation of Eq. (2) under these two constraints, assuming a plasma displacement vanishing at the boundary, is

$$\delta W = \int_{V_p} (\nabla p - \mathbf{j} \times \mathbf{B}) \cdot \boldsymbol{\xi}\, dV. \tag{4}$$

Thus, extremizing W under ideal constraints leads to the force-balance equation $\mathbf{j} \times \mathbf{B} = \nabla p$. In order to uniquely define an equilibrium, in addition to the shape of the plasma boundary, it is required to specify two radial profiles,[14] e.g., the pressure $p(\psi)$ and the rotational transform $\iota(\psi)$ at each flux surface.

The MRxMHD theory was first proposed by Hole, Hudson, and Dewar[17,18] and considers a wider class of plasma equilibria by exploiting the ideas developed by Bhattacharjee and Dewar[19] to generalize the Kruskal-Kulsrud variational principle.[14] In MRxMHD, rather than *continuously* constraining the topology, the topology is *discretely* constrained, thus allowing for partial relaxation. It thus bridges the gap between Taylor's relaxation theory and ideal MHD in a very precise way.[20] Moreover, it allows for the possibility of non-smooth solutions, which are ubiquitous to the three-dimensional MHD problem.

The plasma is partitioned into a finite number N_V of nested volumes $\mathcal{V}_l$, $l = 1, 2, \ldots, N_V$, which undergo Taylor relaxation. These volumes are separated by ideal interfaces $\mathcal{I}_l$, $l = 1, 2, \ldots, N_V - 1$, which are assumed to be magnetic flux surfaces. The energy local to each volume is

$$W_l = \int_{\mathcal{V}_l} \left(\frac{p}{\gamma - 1} + \frac{B^2}{2\mu_0} \right) dV. \tag{5}$$

In each volume $\mathcal{V}_l$, variations are allowed in the pressure, the magnetic field, and the geometry of the interfaces, in order to extremize the local energy W_l. The class of possible variations is defined by certain constraints, which are the discrete equivalents of the continuous constraints imposed in ideal MHD. First, the magnetic field on the interfaces must remain tangential, $\mathbf{B} \cdot \mathbf{n} = 0$, which means that the interfaces are good flux surfaces. Second, the magnetic fluxes in each volume are conserved, which is the discrete equivalent of providing the rotational transform profile, as we shall see later. Third, the magnetic helicity K_l is conserved in each volume $\mathcal{V}_l$, which is the discrete equivalent of the continuous constraint on the helicity in ideal MHD, and a generalization of the single constraint on the global helicity in Taylor's theory. Fourth, the ideal-gas constraint applied to individual fluid elements in ideal MHD is instead applied to each entire relaxed volume, namely, $p_l V_l^\gamma = a_l$, where a_l is a constant and V_l is the volume of $\mathcal{V}_l$. This last constraint is the discrete equivalent of specifying the pressure or mass profile. In order to find MRxMHD equilibria, an energy functional is constructed

$$\mathcal{F} = \sum_l \mathcal{F}_l = \sum_l \left[W_l - \frac{\mu_l}{2}(K_l - K_{l,0}) \right], \tag{6}$$

where W_l is given by Eq. (5) and μ_l is a Lagrange multiplier introduced explicitly to enforce a constant helicity $K_{l,0}$ in each volume $\mathcal{V}_l$. The flux constraints and the tangentiality condition on the interfaces can be enforced implicitly by constraining the representation of the magnetic field or vector potential (see, e.g., Ref. 21 for a more detailed discussion). The first variation of the local, constrained energy functional $\mathcal{F}_l$, is

$$\delta\mathcal{F}_l = \int_{\mathcal{V}_l} (\nabla \times \mathbf{B} - \mu_l \mathbf{B}) \cdot \delta\mathbf{A}\, dV - \int_{\partial\mathcal{V}_l} \left(p_l + \frac{B^2}{2} \right) \cdot \boldsymbol{\xi}\, dV, \tag{7}$$

for arbitrary variations in the field, $\delta\mathbf{B} = \nabla \times \delta\mathbf{A}$, and in the internal interfaces geometry, $\boldsymbol{\xi}$. Therefore, states that extremize the MRxMHD energy functional $\mathcal{F}$ satisfy

$$\nabla \times \mathbf{B} = \mu_l \mathbf{B} \qquad \text{in } \mathcal{V}_l, \tag{8}$$

$$[[p + B^2/2]] = 0 \qquad \text{in } \mathcal{I}_l, \tag{9}$$

where $[[\cdot]]$ denotes the jump across an interface. Equation (8) is a Beltrami equation for the magnetic field and implies complete plasma relaxation in each volume $\mathcal{V}_l$, thus allowing magnetic islands and chaos to form. Equation (9) represents a force-balance condition on the interfaces $\mathcal{I}_l$ and ensures the continuity of total pressure. Both the plasma pressure and magnetic field can nevertheless be discontinuous and therefore both stepped-pressure profiles and singular currents are possible in MRxMHD equilibria. As a matter of fact, by

virtue of Ampere's law, associated with a field discontinuity $[[\mathbf{B}]]$ there is a singular, δ-current density, $\mathbf{j}$, with magnitude $[[\mathbf{B}]] \times \mathbf{n}$, where $\mathbf{n}$ is the unit vector normal to the ideal interface.

As in ideal MHD, in addition to the shape of the plasma boundary, certain quantities must be specified in order to uniquely define a MRxMHD equilibrium. Instead of continuously prescribing the pressure profile as a function of the toroidal flux, the pressure p_l must be prescribed in each volume $\mathcal{V}_l$, together with the amount of enclosed toroidal flux $\Delta\Psi_{t,l}$ in that volume. In addition, both the helicity K_l and the enclosed poloidal flux $\Delta\Psi_p$ must be prescribed in each volume, except for the innermost volume which has a single boundary interface and only the helicity is required. Alternatively, as we shall see later, instead of $(K_l, \Delta\Psi_p)$, it is possible to specify $(\mu_l, \Delta\Psi_p)$ or (ι_l^+, ι_l^-), namely, the rotational transform on the interfaces bounding each volume. This last possibility is clearly the discrete equivalent of specifying the rotational transform profile in ideal MHD. In fact, there is a clear connection between Taylor's relaxation theory, MRxMHD, and ideal MHD. For $N_V = 1$, MRxMHD reduces to Taylor's theory, while ideal MHD is exactly retrieved for $N_V \to \infty$.[20]

Finally, we would like to remark that a close examination of the force-balance condition, Eq. (9), reveals that the existence of ideal interfaces in general three-dimensional equilibria requires the rotational transform on the interfaces to be strongly *irrational*,[22] by which we mean that it satisfies a Diophantine condition.[23] This is consistent with the Kolmogorov-Arnold-Moser (KAM) theorem,[23] which shows that for non-integrable Hamiltonian systems there exists a finite measure of invariant tori provided that the rotational transform is sufficiently irrational. However, this subtle point raises the question of whether it is possible to describe the formation of singular currents at *rational* surfaces within MRxMHD. We expect that this should be possible by virtue of the mathematical proof for the asymptotic convergence of MRxMHD towards ideal MHD.[20] In Secs. III and IV, we shall give a rigorous analytical and numerical proof that this is indeed possible.

III. MODEL FOR ISLAND SHIELDING AND SINGULAR CURRENT FORMATION

Perhaps the simplest but non-trivial examples of current sheets are those in slab geometry. The Hahm-Kulsrud-Taylor model[7] is one such well-known example in which singular currents and magnetic islands are realized as exact solutions of the linearized magnetostatic equations. In this paper, we consider this geometry as a minimum model to describe the shielding of magnetic islands and the subsequent formation of singular currents. We first derive analytically MRxMHD equilibrium states where a magnetic island is produced by a small but resonant magnetic perturbation on the boundary. Then, we look for the analytical limit in which the island is shielded and compute the resulting singular currents forming at the resonant rational surface.

We start by considering a MRxMHD equilibrium for a single-volume, zero-pressure, plasma slab with torus periodicity. We write the position $\mathbf{r} = x\hat{\mathbf{i}} + y\hat{\mathbf{j}} + z\hat{\mathbf{k}}$ with a general set of coordinates (s, θ, ζ), where $\theta, \zeta \in [0, 2\pi]$ and $s \in [-1, 1]$, such that $x = \theta$ and $y = \zeta$ are the two periodic coordinates and $z = R(s, \theta, \zeta)$ is an interpolation between the geometries of the two interfaces defining the boundary of the volume, namely, $R(\pm 1, \theta, \zeta)$. In the simplest case of an unperturbed boundary, we have $R(s, \theta, \zeta) = R_0(1-s)/2 + R_1(1+s)/2$, where R_0 and R_1 give the position of the two interfaces and are assumed to be given.

The magnetic field in the relaxed volume satisfies $\nabla \times \mathbf{B} = \mu\mathbf{B}$ with topological constraints $\mathbf{B} \cdot \nabla s = 0$ at the two interfaces, and the general solution in these coordinates is simply $\mathbf{B} = (B_s, B_\theta, B_\zeta) = (0, B_0 \sin(\bar{\mu}s) + \hat{B}_0 \cos(\bar{\mu}s), B_0 \cos(\bar{\mu}s) - \hat{B}_0 \sin(\bar{\mu}s))$ in the contravariant basis. Here, $\bar{\mu} = \mu\Delta/2$ with $\Delta = R_1 - R_0$, and B_0, $\hat{B}_0$ are two arbitrary constants. The equilibrium state is thus uniquely determined by three constants, namely, $(\bar{\mu}, B_0, \hat{B}_0)$. Similarly to Ref. 13, these three constants can be directly related to the enclosed toroidal and poloidal fluxes, $\Delta\Psi_t = 2\pi B_0 \Delta \sin\bar{\mu}/\bar{\mu}$ and $\Delta\Psi_p = 2\pi\hat{B}_0\Delta \sin\bar{\mu}/\bar{\mu}$, and the volume helicity $K = 2\pi^2(B_0^2 + \hat{B}_0^2)\Delta^2/\bar{\mu} = (\Delta\Psi_t^2 + \Delta\Psi_p^2)\bar{\mu}/(2\sin^2\bar{\mu})$, which is invariant to single-valued gauge transformations. In Ref. 13, however, the relaxed volume is a cylinder with one single outer interface, and thus only two constants, $\Delta\Psi_t$ and K, are required to determine the solution. The rotational transform on the interfaces, $\iota^\pm$, can also be related to the three constants $(\bar{\mu}, B_0, \hat{B}_0)$, as $\iota^\pm = B_\theta(\pm 1)/B_\zeta(\pm 1)$. Therefore, the equilibrium state can be obtained by providing different triplets of constants, e.g., $(\bar{\mu}, B_0, \hat{B}_0)$, $(\Delta\Psi_t, \Delta\Psi_p, K)$, or $(\Delta\Psi_t, \iota^+, \iota^-)$.

With the purpose of building a simple equilibrium state with a resonant rational surface, we choose $\iota^- = -\iota^+$, which is equivalent to setting $\hat{B}_0 = 0$ or $\Delta\Psi_p = 0$.[7] In doing so, we allow for the existence of a rational surface $\iota = 0$, which is resonant to any toroidally symmetric perturbation ($n = 0$, $m \neq 0$). As a matter of fact, in the case of an unperturbed boundary, the magnetic field displays good flux surfaces everywhere (Fig. 1), and the rotational transform profile can be easily computed, $\iota(s) = \tan(\bar{\mu}s)$, thus $\iota(0) = 0$.

We are now in the position to consider a resonant perturbation at the boundaries and to calculate the new equilibrium state which should display an island around the resonant rational surface. The perturbed boundaries are described through their surface geometry, $R(-1, \theta, \zeta) = \sum_{m=0}^{\infty} R_{0,m} \cos(m\theta)$ and $R(+1, \theta, \zeta) = \sum_{m=0}^{\infty} R_{1,m} \cos(m\theta)$, where only $n = 0$ perturbations are considered in order to select a single resonant rational surface $\iota_{res} = n/m = 0$. For the sake of simplicity (we target the minimum model for the generation and shielding of magnetic islands), we consider only the $m = 0, 1$ components.

This perturbation alters the metric elements and the Jacobian, thus complicating the equation $\nabla \times \mathbf{B} = \mu\mathbf{B}$, but a solution can be found analytically in the limit of small perturbations: $R_{0,1}, R_{1,1} \ll \Delta$, where $\Delta = R_{1,0} - R_{0,0}$. In this limit, the general solution is of the form

$$\mathbf{B} = \mathbf{B}_u + (b_s \sin\theta, b_\theta \cos\theta, b_\zeta \cos\theta), \tag{10}$$

where $\mathbf{B}_u$ is the unperturbed solution and $b_s(s)$, $b_\theta(s)$, and $b_\zeta(s)$ are to be found by inserting Eq. (10) into the Beltrami

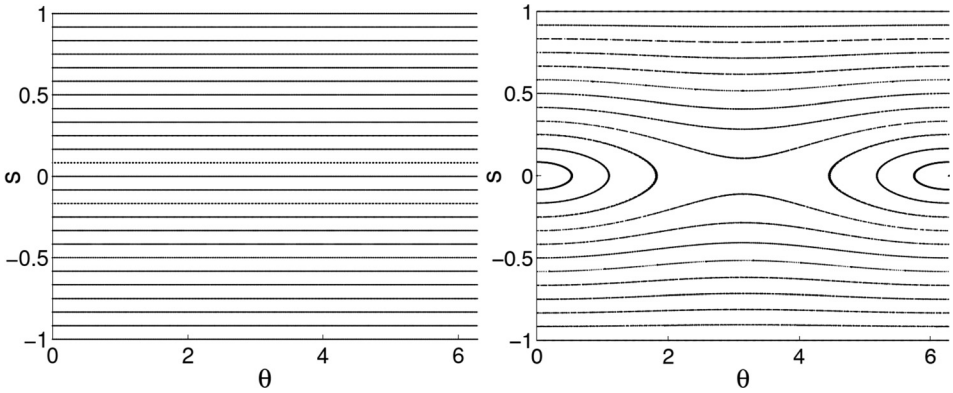

FIG. 1. Poincaré plot of the magnetic field trajectories at fixed $\zeta = 0$, for a single-volume MRxMHD equilibrium state. Left: $R_{0,1} = R_{1,1} = 0$. Right: $R_{0,1} = -10^{-2}$, $R_{1,1} = 10^{-2}$. Results obtained from the analytical solution for $\mathbf{B}$, with $\Delta\Psi_t = 1$, $\iota^{\pm} = \pm 1.618$, and $\Delta = 1$.

equation. In doing so, we use the general relation $(\nabla \times \mathbf{B}) \cdot \mathbf{e}_\delta = \sqrt{g}^{-1} \partial_\alpha B_\beta \, \varepsilon^{\alpha\beta\gamma} g_{\gamma\delta}$, where $\varepsilon^{\alpha\beta\gamma}$ is the Levi-Civita tensor and $g_{\gamma\delta} \equiv \mathbf{e}_\gamma \cdot \mathbf{e}_\delta = \partial_\gamma \mathbf{r} \cdot \partial_\delta \mathbf{r}$ is the metric tensor, whose elements are computed by differentiating the position vector with respect to the coordinates (s, θ, ζ). The problem reduces to a second order, ordinary differential equation for $b_\zeta(s)$

$$b_\zeta'' + \lambda b_\zeta = G(s)\,, \tag{11}$$

with boundary condition $b_\zeta(\pm 1) = 0$, which results from $\mathbf{B} \cdot \nabla s = 0$ at the two interfaces. Here, $\lambda = \bar{\mu}^2 - \Delta^2/4$ and the function $G(s)$ measures the external perturbation, $G(s) = \bar{\mu}\Delta^2/4[\epsilon_0(1-s) + \epsilon_1(1+s)]B_{\theta,u} - 2\bar{\mu}^2(\epsilon_1 - \epsilon_0)B_{\zeta,u}$, where $\epsilon_l = R_{l,1}/\Delta \ll 1$. The solution of Eq. (11) depends on the sign of λ and is given in Appendix A, together with the corresponding expressions for $b_s(s)$ and $b_\theta(s)$. In all cases, however, the equilibrium state is now uniquely determined by a set of six constants, e.g., $(\bar{\mu}, B_0, \hat{B}_0, \Delta, \epsilon_0, \epsilon_1)$. Provided that $\epsilon_0 \neq \epsilon_1$, a Poincaré plot of the magnetic field line trajectories reveals the existence of an island (Fig. 1). We remark that this single-volume MRxMHD equilibrium state corresponds to the fully relaxed Taylor state. As before, we can relate the enclosed toroidal flux, $\Delta\Psi_t$, and the rotational transform on the interfaces, $\iota^{\pm}$, to the constants $(\bar{\mu}, B_0, \hat{B}_0)$. Interestingly, the corresponding expressions are, to first order in ϵ, the same as in the unperturbed system (see Appendix B). Therefore, the equilibrium state may be determined by providing, $(\bar{\mu}, B_0, \hat{B}_0, \Delta, \epsilon_0, \epsilon_1)$ or $(\Delta\Psi_t, \iota^+, \iota^-, \Delta, \epsilon_0, \epsilon_1)$.

With the purpose of approaching the ideal MHD limit in which the island is shielded by the topological constraints and a singular current appears at the resonant rational surface, we now consider that the equilibrium state we have constructed consists of multiple relaxed volumes. In doing so, we can enforce $N_V - 1$ ideal interfaces to exist inside the boundaries of the system, with N_V being the number of relaxed volumes. Theoretically, in the limit $N_V \to \infty$, we know that MRxMHD converges to ideal MHD.[20] However, as we show now, in the zero-pressure limit, both island shielding and singular current formation can be obtained with $N_V = 3$. In fact, with $N_V - 1 = 2$ internal interfaces, we can squeeze the island by bringing them arbitrarily close to the resonant rational surface, thus retrieving the ideal MHD equilibrium state with zero pressure.

We consider three volumes $\mathcal{V}_l$, $l = 1$, 2, and 3. In each volume, $s \in [-1, 1]$, and $\theta, \zeta \in [0, 2\pi]$. The function $R_l(s, \theta, \zeta)$ is given at the interfaces by

$$R_l(s,\theta) = \begin{cases} R_{l,0} + R_{l,1}\cos\theta & \text{if } s = +1 \\ R_{l-1,0} + R_{l-1,1}\cos\theta & \text{if } s = -1 \end{cases}, \tag{12}$$

where $(R_{0,0}, R_{0,1}, R_{3,0}, R_{3,1})$ define the geometry of the boundary interfaces and are assumed to be given. The remaining constants $(R_{1,0}, R_{1,1}, R_{2,0}, R_{2,1})$ define the geometry of the internal interfaces and are unknown *a priori*. Their values are determined by the force-balance condition, which is $[[B^2]] = 0$ across each internal interface. The solution for the magnetic field in each relaxed volume $\mathcal{V}_l$ is given by Eq. (10) together with Eq. (A7), and its dependence is as follows:

$$\mathbf{B}_l = \mathbf{B}_l(B_{0l}, \hat{B}_{0l}, \bar{\mu}_l, \Delta_l, \epsilon_{l-1}, \epsilon_l), \tag{13}$$

for $l = 1$, 2, and 3, and where $\Delta_l = R_{l,0} - R_{l-1,0}$, $\epsilon_{l-1} = R_{l-1,1}/\Delta_l$, and $\epsilon_l = R_{l,1}/\Delta_l$. After providing the geometry of the boundaries and the triplet $(\Delta\Psi_{t,l}, \iota_l^+, \iota_l^-)$ for each volume $\mathcal{V}_l$, the geometries of the internal interfaces remain undetermined, and the self-consistent equilibrium solution for $\mathbf{B}_l$ is found by enforcing the force-balance condition, $[[B^2]] = 0$, across each internal interface. Keeping, as before, only first order terms in the geometrical perturbation amplitudes, ϵ_l, the force-balance condition can be written as $[[B^2]]_{m=0} + [[B^2]]_{m=1}\cos\theta = 0$, and since the two components must vanish independently, this gives four constraints in total (two per interface). More precisely, the $m = 0$ and $m = 1$ components of the force-balance conditions at the two internal interfaces lead to two decoupled linear systems whose solutions provide, respectively, expressions for (Δ_1, Δ_2) and $(R_{1,1}, R_{2,1})$, thus uniquely determining $\mathbf{B}_l$. A detailed derivation is given in Appendix C. Figure 2 shows an example of Poincaré plot for a three-volume MRxMHD equilibrium state (with and without perturbation) computed from the analytical solution for the magnetic field. We remark that the positions and geometries of the internal interfaces are not imposed. They are self-consistently computed from the force-balance condition. However, there is freedom in setting the outer boundary geometries, the enclosed toroidal fluxes in each relaxed volume, and the rotational transform on each interface.

The area that each volume $\mathcal{V}_l$ occupies in a Poincaré section is proportional to the enclosed toroidal flux, given

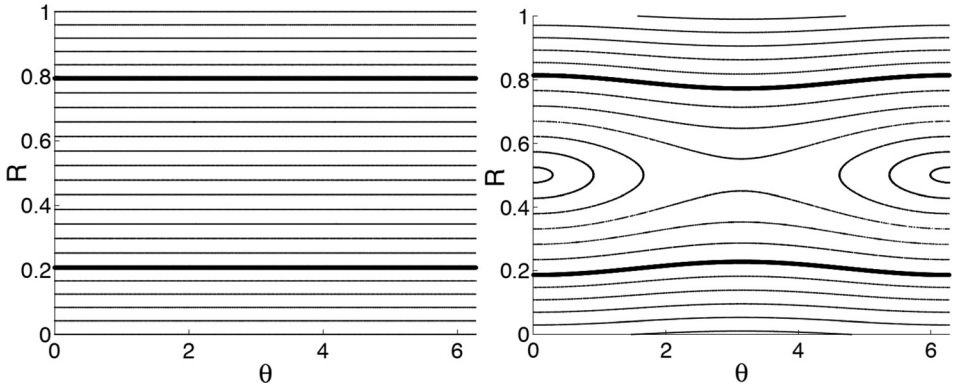

FIG. 2. Poincaré plot of the magnetic field trajectories at fixed $\zeta = 0$, for a three-volume MRxMHD equilibrium state. Left: $R_{0,1} = R_{3,1} = 0$. Right: $R_{0,1} = -10^{-2}$, $R_{3,1} = 10^{-2}$. Thick lines indicate the internal interfaces. Results obtained from the analytical solution for $\mathbf{B}$, with fluxes $\Delta\Psi_{t,1} = \Delta\Psi_{t,3} = 0.1695$, $\Delta\Psi_{t,2} = 0.6610$, and rotational transforms $\iota_1^- = -1.618$, $\iota_1^+ = \iota_2^- = -0.679$, $\iota_2^+ = \iota_3^- = 0.679$, and $\iota_3^+ = 1.618$. System size is $\Delta_1 + \Delta_2 + \Delta_3 = 1$.

that $\Delta\Psi_{t,l} = 2\pi B_{0l}\Delta_l \sin\bar{\mu}_l/\bar{\mu}_l$ and that Δ_l is the average separation between the two interfaces defining the volume $\mathcal{V}_l$. Therefore, a sequence of MRxMHD equilibrium states in which the enclosed toroidal flux $\Delta\Psi_{t,2}$ approaches zero and the rotational transform on the internal interfaces, ι_2^- and ι_2^+, approach the resonant value $\iota_{res} = 0$, should squeeze the island and make it vanish, thus retrieving the ideal MHD limit. The vanishing of the island should occur if the $m = 1$ components of the internal interfaces deformation, $R_{1,1}$ and $R_{2,1}$, converge to the same finite value when $\Delta\Psi_{t,2}$, $\iota_2^\pm \to 0$. However, as shown in Appendix C, the solution for the interfaces deformation is $\mathbf{R} = \mathcal{M}^{-1}\mathbf{S}$ and both $\det(\mathcal{M})$ and $\mathbf{S}$ go to zero when $\Delta\Psi_{t,2}, \iota_2^\pm \to 0$. Thus, in the same way that $\lim_{x,y\to 0} x/y$ is not defined unless the rate at which x and y approach zero is specified, we need to specify the exact way $\iota_2^\pm$ and $\Delta\Psi_{t,2}$ approach zero. For the particular case of an unperturbed, single relaxed volume, both quantities approach zero at the same rate, but here we may consider more general limits. Consider then

$$\iota_2^\pm = \pm X^\alpha, \tag{14}$$

$$\Delta\Psi_{t,2} = X^\beta, \tag{15}$$

where α, $\beta > 0$, and $X \to 0$. The self-consistent solution for the geometry of the internal interfaces is then

$$\lim_{X\to 0}\Delta_1 = \lim_{X\to 0}\Delta_3 = 1/2\,, \quad \lim_{X\to 0}\Delta_2 = 0\,, \tag{16}$$

$$\lim_{X\to 0} R_{1,1} = \lim_{X\to 0} R_{2,1} = \frac{\kappa}{2}(R_{0,1} + R_{3,1}), \tag{17}$$

for $\beta > \alpha$, and where $\kappa \in [0, 1]$ depends on the magnitude of the rotational transform on the external interfaces and its exact expression is given in Appendix C. Equation (17) implies that for $\beta > \alpha$ the magnetic island should vanish. This result provides a precise way to shield the island forming around the resonant rational surface and thus to retrieve the ideal MHD limit in which singular currents are expected to develop.

Figure 3 shows an example of a sequence of MRxMHD equilibrium states with decreasing X and where $\alpha = 1$ and $\beta = 2.5$ have been chosen. As expected, the island is squeezed and the magnitudes of $R_{1,1}$ and $R_{2,1}$ converge to the same value, as shown in Fig. 4. Notice that in both Figs. 2 and 3 there is a $m = 1$ and $n = 0$ island forming around the resonant rational surface, but with a different poloidal phase. This is simply due to the fact that the signs of $R_{1,1}$ and $R_{2,1}$ are reversed.

We remark that for $\beta \le \alpha$, however, $R_{1,1}$ and $R_{2,1}$ converge to different values (see Appendix C) and thus the interfaces intersect each other, indicating that in this case the assumed geometrical description of the interfaces is not sufficient. This suggests that other MRxMHD equilibrium solutions with non-trivial geometry may exist. As a matter of fact, plasmoid solutions to the same equilibrium problem have been constructed in a recent publication.[24] Despite this apparent non-uniqueness of solutions, which deserves further investigation, we target here the particular limit of ideal MHD, which excludes plasmoid-like solutions.

The limit defined above, Eqs. (16) and (17), corresponds to the ideal MHD limit, since the island vanishes completely and magnetic flux surfaces are present everywhere. As predicted by ideal MHD, we expect a δ-current forming at the resonant rational surface, which corresponds here to the two coinciding interfaces. This singular current density arises naturally because of a discontinuity in the tangential magnetic field. More precisely, we have that

$$\mathbf{j} = [[\mathbf{B}]] \times \mathbf{n}\,\delta(\iota - \iota_{res}), \tag{18}$$

where $\mathbf{n}$ is the unit vector normal to the magnetic flux surface and here $[[\mathbf{B}]] = \mathbf{B}_3(s = -1) - \mathbf{B}_1(s = +1)$, since the volume $\mathcal{V}_2$ vanishes in the limit $X \to 0$. We can write an analytical expression for the discontinuity, $[[\mathbf{B}]]$, by using Eq. (10) in the limit defined by Eqs. (16) and (17). We must distinguish the two cases $\mu > 1$ and $\mu < 1$ for which the solution of the Beltrami equation is different, although the transition from one solution to the other at $\mu = 1$ is smooth (see Appendix A). In both cases,

$$\lim_{X\to 0}[[B_\zeta]] = 0\,, \tag{19}$$

$$\lim_{X\to 0}[[B_\theta]] = [[b_\theta]]\cos\theta \neq 0, \tag{20}$$

where b_θ can be expressed using Eq. (A7). This indicates that there is a singular δ-current density along the ζ direction and with a poloidal average of zero. For $\mu > 1$,

$$[[b_\theta]] = \frac{2kB_0 \sin\bar{\mu}}{\Delta}(\tan k + \cot k)(R_{0,1} - R_{3,1}), \tag{21}$$

where $B_0 \equiv B_{01}$, $\bar{\mu} \equiv \bar{\mu}_1$, $\Delta \equiv \Delta_1$, $k \equiv k_1$ and we have used $R_{1,1} = R_{2,1}$. For $\mu < 1$,

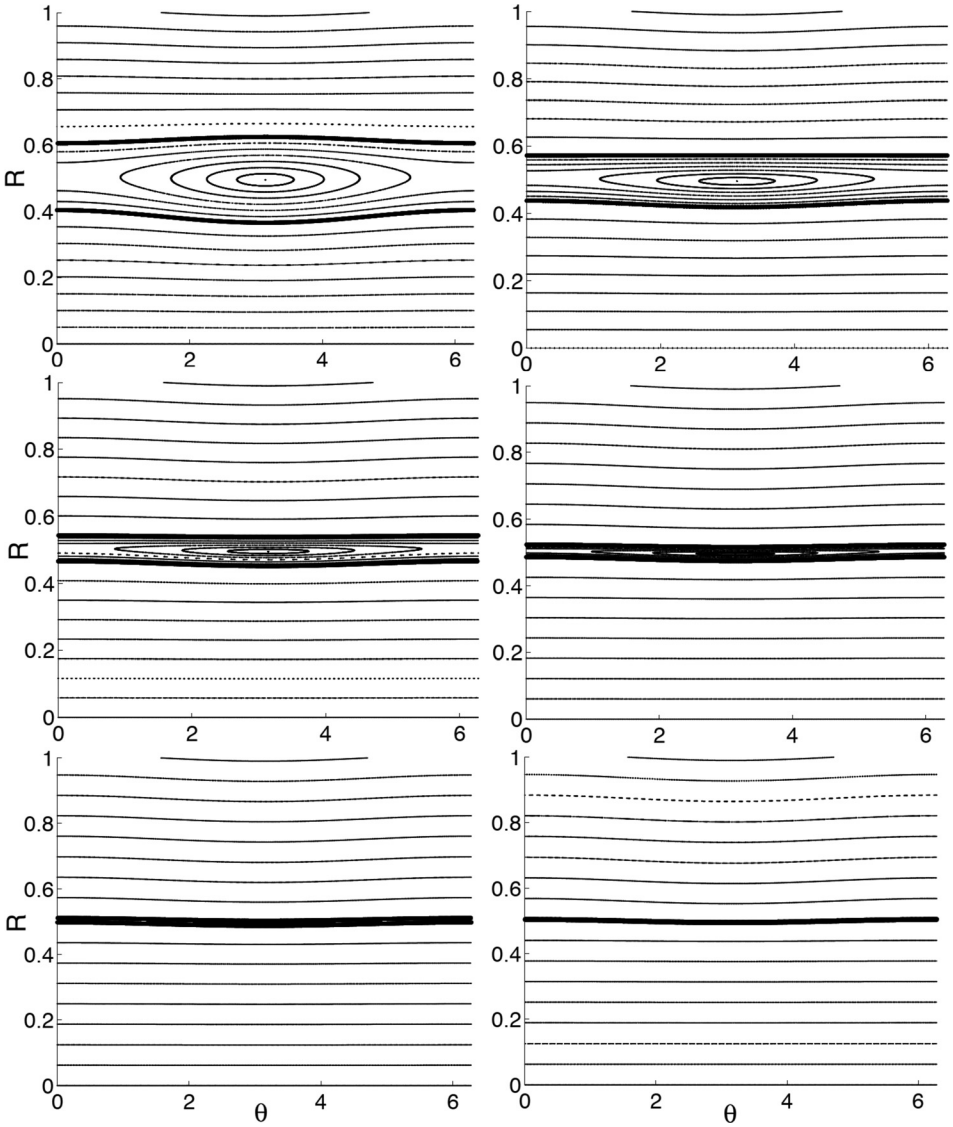

FIG. 3. Sequence of MRxMHD equilibrium states with decreasing $X \in [0.1, 0.6]$ with $\alpha = 1$ and $\beta = 2.5$. Here, the boundary perturbations are $R_{0,1} = 0$ and $R_{3,1} = 1 \times 10^{-2}$. In the bottom right panel equilibrium, we have $\Delta_2 = 2.61 \times 10^{-3}$, $R_{1,1} = 4.97 \times 10^{-3}$, and $R_{2,1} = 4.55 \times 10^{-3}$; therefore, $|R_{2,1} - R_{1,1}|/\Delta_2 \approx 0.1 < 1$ ensures no crossing.

$$[[b_\theta]] = \frac{2kB_0 \sin\bar{\mu}}{\Delta} \frac{2}{\sinh 2k} (R_{0,1} - R_{3,1}) . \tag{22}$$

Figure 5 confirms the presence of such a δ-current density in the ideal MHD limit. A prediction of the magnitude of the δ-current is therefore possible by using MRxMHD to compute the discontinuity in the tangential field that remains when the island is shielded in between two ideal interfaces.

We can retrieve the Hahm-Kulsrud-Taylor (HKT) solution for the δ-current,[7] by taking the limit of small $\bar{\mu}$ in Eq. (22), identifying $a \equiv \Delta$ and $2\delta \equiv (R_{0,1} - R_{3,1})$, which gives

$$[[B_\theta]] = \frac{2\bar{\mu}B_0}{\sinh a} 2\delta \cos\theta \tag{23}$$

and by noticing that $2\bar{\mu}B_0$ is equal to the poloidal field at the outer boundary, $B_{\theta 3}(s = +1)$, which is labeled 'B_0' in Ref. 7.

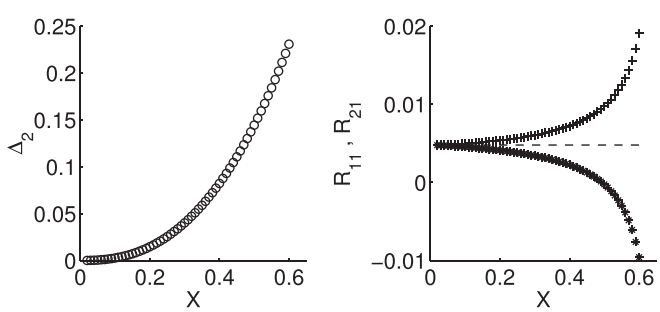

FIG. 4. Geometrical parameters of the inner volume $\mathcal{V}_2$ as a function of the sequence parameter X. On the right panel, $R_{1,1}$ (crosses) and $R_{2,1}$ (stars) converge to the theoretical value (dashed line) computed from Eq. (17).

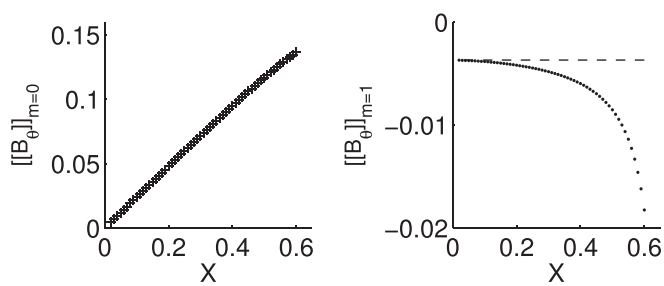

FIG. 5. Discontinuity in the poloidal field as a function of the sequence parameter X. Left: $m = 0$ component, which is expected to be zero in the limit $X \to 0$, see Eq. (20). Right: $m = 1$ component, expected to be finite in the limit $X \to 0$, with a theoretical value given by Eq. (21) (dashed line).

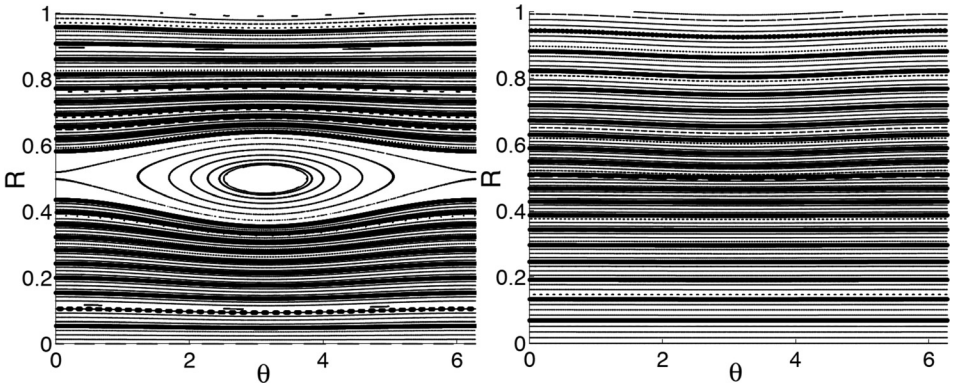

FIG. 6. Poincaré plot of the magnetic field line trajectories at fixed $\zeta = 0$, for a MRxMHD equilibrium with $N_V = 21$, $\iota_0 = 1.618$, and $p_0 = 10^{-3}$, and with boundary perturbations $R_{0,1} = 0$ and $R_{3,1} = 1 \times 10^{-2}$. Left: $X = 0.6$, $\alpha = 1$, $\beta = 2.5$. Right: $X = 0.1$, $\alpha = 1$, $\beta = 2.5$.

This shows that the HKT solution is only valid in the limit of small rotational transform, i.e., dominant toroidal field.

Finally, we consider a finite-pressure MRxMHD equilibrium state, with the purpose of describing the formation of pressure-driven singular currents around the resonant rational surface in the ideal MHD limit. For the sake of simplicity, we consider a stepped-approximation to a pressure profile that is linear in toroidal flux, $p(\Psi) = p_0(1 - \Psi)$, $\Psi \in [0, 1]$, with a large number of relaxed volumes, $N_V \gg 1$. Similarly, the rotational transform on the interfaces approximates a linear profile, $\iota(\Psi) = \iota_0(2\Psi - 1)$.

The solution for the magnetic field $\mathbf{B}_l$ in each relaxed volume $\mathcal{V}_l$ is given by Eq. (10) together with Eq. (A7), and its complete knowledge requires solving the multi-volume force-balance equations, Eqs. (C3) and (C4), which provide expressions for the geometry of the internal interfaces, namely, $\{\Delta_l, R_{l,1}\}$.

An example of such an equilibrium is given in Fig. 6, showing that the magnetic island produced by a resonant perturbation can be shielded by following the same procedure as defined previously. More precisely, the enclosed toroidal flux in the innermost volume is $\Delta\Psi_t = X^\beta$ and the rotational transform on the innermost interfaces is $\iota^\pm = \pm X^\alpha$.

As before, a δ-current develops at the rational surface in the limit $X \to 0$, except this time a pressure-driven singular current is also established around the resonant rational surface. Figure 7 shows the formation of such current for finite pressure gradient.

We remark that since MRxMHD is a weak formulation to the MHD problem,[21,25] the local current densities produced by the finite field discontinuities in Fig. 7 should not be interpreted as local singularities; instead, their integral over an arbitrary finite surface gives the total actual current across such surface. This current is expected to be proportional to the pressure gradient $|\nabla p| \equiv p_0$ and to diverge as $1/(\iota - \iota_{res})$. Both properties are confirmed by Fig. 8.

In this section, we have developed an analytical model based on the linearized MRxMHD theory. This model can accurately (1) describe the formation of magnetic islands at resonant rational surfaces, (2) retrieve the ideal MHD limit where magnetic islands are shielded, and (3) compute the subsequent formation of both δ-currents and pressure-driven $1/x$ currents. The model is of course restricted to slab, linearly perturbed equilibrium solutions; however, to our knowledge, this is the first model that can achieve points (1)–(3) at the same time. In the next section, we use a fully nonlinear implementation of the MRxMHD theory to benchmark the analytical results.

IV. NONLINEAR EQUILIBRIUM CALCULATIONS

A numerical implementation of the MRxMHD theory, the Stepped-Pressure Equilibrium Code (SPEC),[21] was recently developed. SPEC is capable of calculating three-dimensional MRxMHD equilibria in slab, cylindrical, and toroidal geometries. SPEC has been benchmarked against VMEC in the axisymmetric case[20,21] and has been used to reproduce self-organized helical states in reversed field pinches.[26]

In this paper, we use SPEC in slab geometry in order to benchmark the obtained nonlinear results against those of the semi-analytical, linear model derived in Sec. III. First, we consider the shielding of a magnetic island in the zero-pressure, $N_V = 3$ case, and the subsequent formation of the singular δ-current density at the rational surface. Figure 9 shows a sequence of Poincaré plots obtained from MRxMHD equilibria computed with SPEC with the exact same input parameters as in Fig. 3. We observe the shielding of the magnetic island around the rational surface, as predicted by the linearized model.

The theoretical predictions derived in Sec. III for the geometry of the internal interfaces and the magnitude of the δ-

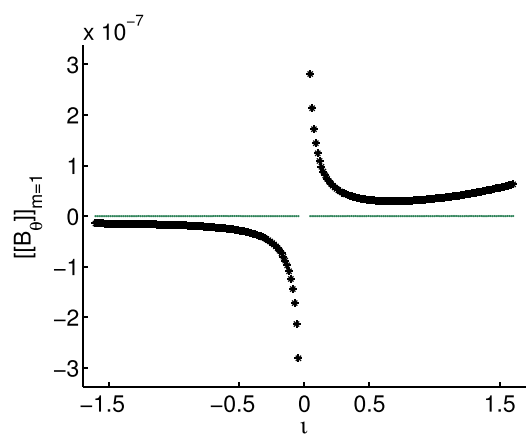

FIG. 7. Discontinuity in the $m = 1$ component of the poloidal field at each interface as a function of the corresponding rotational transform ι for a MRxMHD equilibrium with $N_V = 221$ and $X = 0.05$. A divergent current is established around $\iota_{res} = 0$ for finite pressure gradient ($p_0 = 10^{-3}$, black stars), while it vanishes for zero-pressure ($p_0 = 0$, green dots).

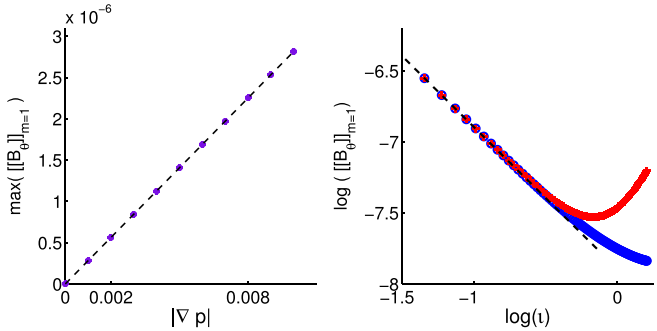

FIG. 8. Left: magnitude of $[[B_\theta]]_{m=1}$ across a fixed interface, as a function of the pressure gradient $|\nabla p| \equiv p_0$, showing a linear relation (black dashed line has slope 1). Right: log-scale plot of the negative (blue circles) and positive (red crosses) sides of the curve in Fig. 7, showing a $1/\iota$ divergence (black dashed line has slope -1) near the resonant rational surface.

current established in the limit of no island, Eqs. (16), (17), and (21), are benchmarked against the results of nonlinear calculations carried out with SPEC. The results of such a convergence study are shown in Figs. 10 and 11. The convergence is clear and as expected the agreement between linear and nonlinear results is improved as the boundary perturbation is decreased.

Finally, we consider the multi-volume calculations with finite pressure gradient. Figure 12 shows the results of SPEC calculations for a MRxMHD equilibrium with $N_V = 63$ volumes, finite pressure gradient, and an island squeezed with $X = 0.04$. The corresponding theoretical predictions of the linearized model are also shown. Both curves confirm the presence of a divergent pressure-driven current around the

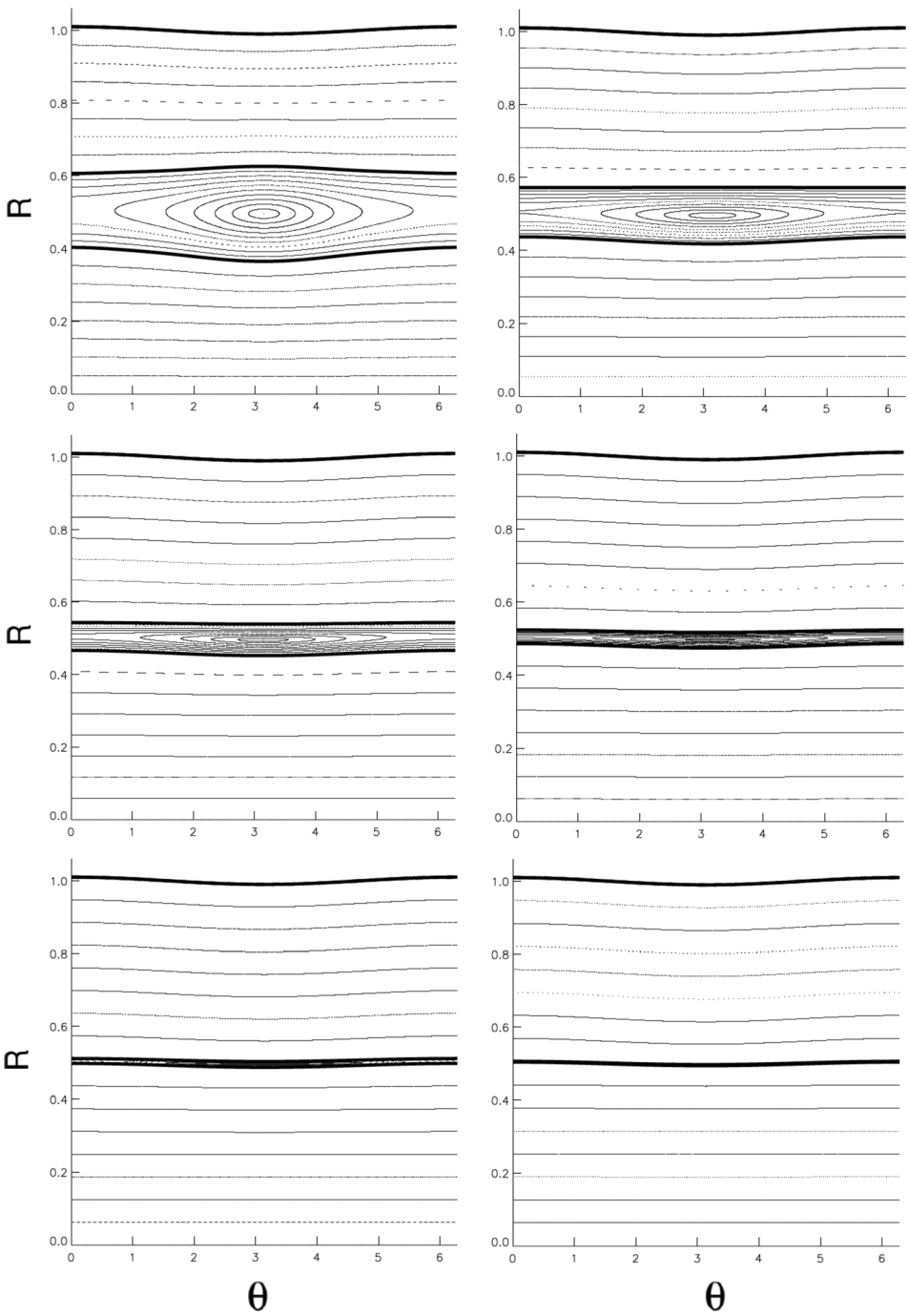

FIG. 9. Sequence of MRxMHD equilibrium states computed from SPEC with decreasing X and where $\alpha = 1$ and $\beta = 2.5$. All input parameters are exactly the same as in Fig. 3.

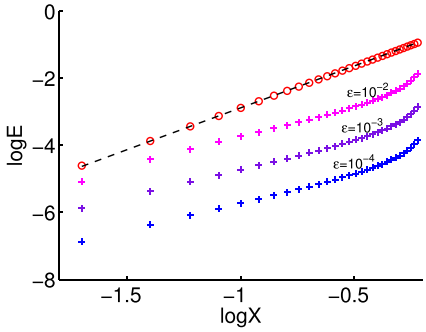

FIG. 10. Convergence of the SPEC results towards the theoretical prediction of the linearized model for the geometry of the internal interfaces, Eqs. (16) and (17), as $X \to 0$. Circles and crosses correspond, respectively, to the errors in the $m=0$ and $m=1$ components of the internal interfaces geometry, namely, $E = |\Delta_1^{SPEC} - 1/2|$ and $E = |R_{1,1}^{SPEC} - \kappa R_{3,1}/2|$. As expected, decreasing the boundary perturbation amplitude, $\epsilon = R_{3,1}$, improves the agreement between the linear and nonlinear results for the $m=1$ component, while the $m=0$ component does not depend on the boundary perturbation. The dashed line has slope β, which is the expected convergence rate for the $m=0$ component of the geometry.

resonant rational surface. As discussed in Sec. III, this current has a $1/\imath$ divergence and a magnitude proportional to the pressure gradient.

V. CONCLUSIONS AND OUTLOOK

In this paper, we have developed an understanding of how MRxMHD can capture the formation of the singular currents that are expected in non-axisymmetric ideal MHD equilibria. A semi-analytical model that considers linearized MRxMHD equilibria in slab geometry has been derived and provides a theoretical framework in which to explore the physics of magnetic island shielding and singular current formation. In particular, the Hahm-Kulsrud-Taylor solution[7] for the magnitude of the δ-current in slab geometry can be retrieved. The model has then been used as a guide to retrieve the ideal MHD limit in nonlinear equilibrium calculations carried out with the SPEC code.

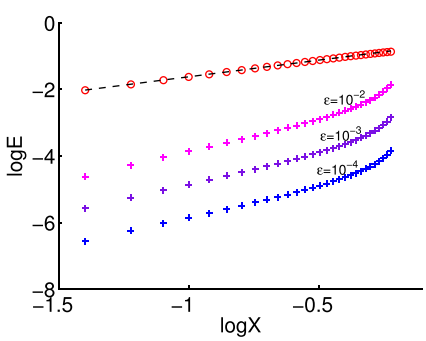

FIG. 11. Convergence of the SPEC results towards the theoretical prediction of the linearized model for the δ-current amplitude, Eq. (21), as $X \to 0$. Circles and crosses correspond, respectively, to the errors in the $m=0$ and $m=1$ components of the field discontinuity, namely, $E = |[[B_\theta]]_{m=0}^{SPEC}|$ and $E = |[[B_\theta]]_{m=1}^{SPEC} + 4kB_0 \sin\bar{\mu}(\tan k + \cot k)R_{3,1}|$. As expected, the agreement between the linear and nonlinear results is improved for the $m=1$ component by decreasing the boundary perturbation amplitude, while the $m=0$ component does not depend on the boundary perturbation. The dashed line has slope α, which is the expected convergence rate for the $m=0$ component of the field discontinuity.

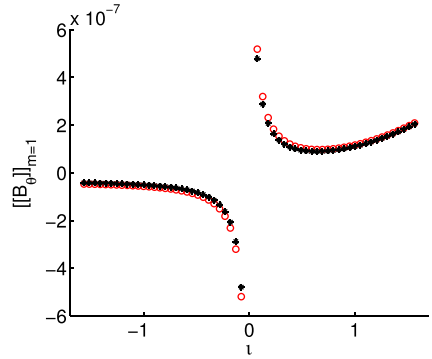

FIG. 12. Discontinuity in the $m=1$ component of the poloidal field at each interface as a function of the corresponding rotational transform $\imath$ for a MRxMHD equilibrium with $N_V = 63$, $R_{3,1} = 10^{-2}$, $p_0 = 10^{-3}$, and $X = 0.04$. A divergent current is established around $\imath_{res} = 0$. Red circles are from SPEC and black stars are from the linearized model.

The results presented here are, to our knowledge, the first nonlinear MHD equilibrium calculations showing the formation of both δ-currents and pressure-driven $1/x$ currents around resonant rational surfaces. Moreover, the results presented here encourage the use of MRxMHD to perform magnetic equilibrium calculations in three-dimensional magnetically confined plasmas, where both magnetic islands and singular currents are expected to exist. In particular, SPEC is capable of computing MRxMHD equilibrium states in slab, cylindrical, and toroidal geometries and thus represents a promising tool for the computation of three-dimensional magnetic equilibria in fusion devices.

In the future, cylindrical MRxMHD equilibria will be considered in order to retrieve the Rosenbluth-Dagazian-Rutherford solution[8,27] for the saturated $m=1$, $n=1$ ideal kink mode and the current sheet associated with it. This should represent a step further in the computation of three-dimensional MHD equilibria with singular currents in toroidal geometry. Also, the presence of secondary islands around a shielded rational surface,[28,29] which are compatible with MRxMHD, will be studied. Finally, the possibility of magnetic island shielding with a single ideal interface presenting a discontinuous rotational transform will be explored. This is motivated by the results of Appendix C, which suggest that the only sequence ensuring no overlapping of interfaces is one with $\alpha = 0$, $\beta > 0$, thus leading to a discontinuous transform.

ACKNOWLEDGMENTS

We acknowledge discussions with Robert Dewar and Joachim Geiger. This work was carried out under the auspices of the Max-Planck-Princeton Center for Plasma Physics.

APPENDIX A: SINGLE-VOLUME, PERTURBED SOLUTION

The general solution to Eq. (11) is the sum of the homogeneous solution and a particular solution to Eq. (11)

$$b_\zeta(s) = ay(s) + \hat{a}\hat{y}(s) - \bar{\mu}[\epsilon_0(1-s) + \epsilon_1(1+s)]B_{\theta,u}, \quad \text{(A1)}$$

where $a, \hat{a}$ are constants and $\{y, \hat{y}\}$ is the basis of functions for the homogeneous solution

$$\{y,\hat{y}\} = \begin{cases} \{\cos(ks),\ \sin(ks)\} & \text{if } \lambda \geq 0 \\ \{e^{ks}, e^{-ks}\} & \text{if } \lambda < 0, \end{cases} \tag{A2}$$

with $k \equiv \sqrt{|\lambda|}$. Imposing the boundary conditions, $b_\zeta(\pm 1) = 0$, we find a and $\hat{a}$. For $\lambda \geq 0$, or equivalently $\mu \geq 1$, we have

$$a = \frac{\bar{\mu}}{\cos k}\left(\epsilon_1 B_{\theta,u}(1) + \epsilon_0 B_{\theta,u}(-1)\right), \tag{A3}$$

$$\hat{a} = \frac{\bar{\mu}}{\sin k}\left(\epsilon_1 B_{\theta,u}(1) - \epsilon_0 B_{\theta,u}(-1)\right), \tag{A4}$$

and for $\lambda < 0$, or equivalently $\mu < 1$, we have

$$a = \frac{\bar{\mu}}{\sinh(2k)}\left(\epsilon_1 B_{\theta,u}(1)e^{k} - \epsilon_0 B_{\theta,u}(-1)e^{-k}\right), \tag{A5}$$

$$\hat{a} = -\frac{\bar{\mu}}{\sinh(2k)}\left(\epsilon_1 B_{\theta,u}(1)e^{-k} - \epsilon_0 B_{\theta,u}(-1)e^{k}\right). \tag{A6}$$

The three components of the perturbed solution for the magnetic field, which are coupled via the Beltrami equation, are then

$$\begin{aligned} b_s &= -\frac{\Delta^2}{4\bar{\mu}}\left(a y_1(s) + \hat{a} y_2(s)\right), \\ b_\theta &= -\frac{1}{\bar{\mu}}\left(a y_1'(s) + \hat{a} y_2'(s)\right) + \bar{\mu}\left[\epsilon_0(1-s) + \epsilon_1(1+s)\right] B_{\zeta,u}, \\ b_\zeta &= a y_1(s) + \hat{a} y_2(s) - \bar{\mu}\left[\epsilon_0(1-s) + \epsilon_1(1+s)\right] B_{\theta,u}, \end{aligned} \tag{A7}$$

and are uniquely determined by the parameters $(\bar{\mu}, B_0, \hat{B}_0, \Delta, \epsilon_0, \epsilon_1)$. Equation (A7) satisfies the Beltrami equation, $\nabla \times \mathbf{B} = \mu \mathbf{B}$, up to first order in ϵ.

APPENDIX B: TOROIDAL FLUX AND ROTATIONAL TRANSFORM

The rotational transform on the interfaces is given by

$$\begin{aligned} \dot{\theta}^{\pm} &\equiv \left.\frac{\mathbf{B}\cdot\nabla\theta}{\mathbf{B}\cdot\nabla\zeta}\right|_{s=\pm 1} \\ &= \left.\frac{B_{\theta,u}(s) + b_\theta(s)\cos\theta}{B_{\zeta,u}(s) + b_\zeta(s)\cos\theta}\right|_{s=\pm 1}, \end{aligned} \tag{B1}$$

where the magnetic field components are given by Eq. (10) together with Eq. (A7). In particular, we have that $b_\zeta(s=\pm 1) = 0$. Equation (B1) is a function of θ and therefore a "local" quantity. We can however introduce a straight-field-line angle, $\theta_s = \theta + w\sin\theta$, with $w \sim \epsilon$ such that

$$\left.\frac{\mathbf{B}\cdot\nabla\theta_s}{\mathbf{B}\cdot\nabla\zeta}\right|_{s=\pm 1} \equiv \text{ɨ}^{\pm} \tag{B2}$$

is a constant. This constrains the value of w

$$\begin{aligned} \text{ɨ}^{\pm} &= \left.\frac{\mathbf{B}\cdot\nabla\theta}{\mathbf{B}\cdot\nabla\zeta}\right|_{s=\pm 1}\frac{d\theta_s}{d\theta} \\ &= \frac{B_{\theta,u}(\pm 1)}{B_{\zeta,u}(\pm 1)} + \frac{w B_{\theta,u}(\pm 1) + b_\theta(\pm 1)}{B_{\zeta,u}(\pm 1)}\cos\theta + O(\epsilon^2), \end{aligned} \tag{B3}$$

giving $w^{\pm} = -b_\theta(\pm 1)/B_{\theta,u}(\pm 1)$ and therefore the rotational transform is, to first order in ϵ

$$\text{ɨ}^{\pm} = \frac{B_{\theta,u}(\pm 1)}{B_{\zeta,u}(\pm 1)} = \frac{\pm B_0 \sin(\bar{\mu}) + \hat{B}_0\cos(\bar{\mu})}{B_0\cos(\bar{\mu}) \mp \hat{B}_0 \sin(\bar{\mu})}, \tag{B4}$$

which is the unperturbed rotational transform.

The enclosed toroidal flux in the volume is given by

$$\begin{aligned} \Delta\psi_t &= \int_\Sigma \mathbf{B}\cdot\mathbf{d}\sigma \\ &= \int_0^{2\pi}\int_{-1}^{1} \mathcal{J}(s,\theta) B^\zeta(s,\theta)\, ds\, d\theta \\ &= \frac{\Delta}{2}\int_0^{2\pi}\int_{-1}^{1}\left(1 + (\epsilon_1 - \epsilon_0)\cos\theta\right)\left(B_{\zeta,u}(s) + b_\zeta(s)\cos\theta\right) ds\, d\theta \\ &= 2\pi B_0 \Delta \sin\bar{\mu}/\bar{\mu} + O(\epsilon^2), \end{aligned} \tag{B5}$$

where $\mathcal{J} = \sqrt{g}$ is the Jacobian. Equation (B5) is, to first order in ϵ, the unperturbed toroidal flux.

APPENDIX C: MULTI-VOLUME, FORCE-BALANCE CONDITION

Assume that $(\Delta\psi_{t,l}, \text{ɨ}_l^+, \text{ɨ}_l^-, p_l)$ are provided in each volume, as well as the system size $L_{sys} = \sum_{l=1}^{N_V}\Delta_l$. Inverting Eqs. (B4) and (B5), we can determine $(\bar{\mu}_l, Q_l, \hat{Q}_l)$, where $Q_l \equiv B_{0l}\Delta_l$ and $\hat{Q}_l \equiv \hat{B}_{0l}\Delta_l$. Then, the parameters that need to be determined in order to uniquely define the solution for $\mathbf{B}$ are $\{\Delta_l, R_{l,1}\}$ for $l = 1,\ldots N_V$, and these can be computed by solving the force-balance condition, which is

$$\left[\left[p + \frac{B^2}{2}\right]\right] = 0, \tag{C1}$$

where $[[x]] = x_{l+1}(s=-1) - x_l(s=+1)$ is the difference in x between the outer side and the inner side of each internal interface separating volumes $\mathcal{V}_l$ and $\mathcal{V}_{l+1}$. We thus need to compute the quantity $\mathbf{B}_l^2$ on the interfaces, which is

$$\begin{aligned} \mathbf{B}_l^2(\pm 1,\theta) &= B_\theta^2(\pm 1,\theta) + B_\zeta^2(\pm 1,\theta) + O(\epsilon^2) \\ &= f_{l,0} + 2\cos\theta f_{l,1}^{\pm} + O(\epsilon^2), \end{aligned} \tag{C2}$$

where $f_{l,0} = B_{0l}^2 + \hat{B}_{0l}^2$ and $f_{l,1}^{\pm} = B_{\theta,u}(\pm 1) b_\theta(\pm 1)$, which can be written in terms of $(\bar{\mu}_l, Q_l, \hat{Q}_l)$ and the yet-not-determined geometrical parameters $\{\Delta_l, R_{l,1}\}$, with $l = 1,\ldots N_V$.

The $m = 0$ component of the force-balance condition across each interface, which is $2p_l + f_{l,0} = 2p_{l+1} + f_{l+1,0}$ can be written as

$$\begin{aligned} &2(p_l - p_{l+1})\Delta_l^2\Delta_{l+1}^2 + (Q_l^2 + \hat{Q}_l^2)\Delta_{l+1}^2 \\ &\quad - (Q_{l+1}^2 + \hat{Q}_{l+1}^2)\Delta_l^2 = 0 \end{aligned} \tag{C3}$$

and consists of a nonlinear system of $N_V - 1$ equations for $\{\Delta_l\}$, although the system becomes linear in the zero-pressure limit.

The $m = 1$ component of the force-balance condition across each interface, which is $f_{l,1}^+ = f_{l+1,1}^-$, can be written as

$$(\mathcal{C}_l^+ - \mathcal{C}_{l+1}^-)R_{l,1} + \mathcal{D}_{l+1}R_{l+1,1} + \mathcal{D}_l R_{l-1,1} = 0 \tag{C4}$$

and consists of a linear system of $N_V - 1$ equations for $\{R_{l,1}\}$, where $\mathcal{C}_l^{\pm}$ and $\mathcal{D}_l$ are defined as

$$\mathcal{C}_l^{\pm} = \pm\frac{k_l}{\Delta_l^3}\left(Q_l \sin\bar{\mu}_l \pm \hat{Q}_l \cos\bar{\mu}_l\right)^2 (\tan k_l - \cot k_l) + \frac{\bar{\mu}_l}{\Delta_l^3}\left[\pm\left(Q_l^2 - \hat{Q}_l^2\right)\sin 2\bar{\mu}_l + 2Q_l\hat{Q}_l \cos 2\bar{\mu}_l\right], \quad \text{(C5)}$$

$$\mathcal{D}_l = \frac{k_l}{\Delta_l^3}\left(\hat{Q}_l^2 \cos^2\bar{\mu}_l - Q_l^2 \sin^2\bar{\mu}_l\right)(\tan k_l + \cot k_l), \quad \text{(C6)}$$

for $\mu_l > 1$ and similarly for $\mu_l < 1$. The system (C4) can be written as a matrix equation

$$\mathcal{M}\mathbf{R} = \mathbf{S}, \quad \text{(C7)}$$

where $\mathbf{R} = (R_{1,1}, R_{2,1}, \ldots, R_{N_V-1,1})$ and $\mathcal{M}$, $\mathbf{S}$ are known once the system (C3) has been solved. More precisely, $\mathbf{S} = (-\mathcal{D}_1 R_{0,1}, 0, \ldots, 0, -\mathcal{D}_{N_V} R_{N_V,1})$ and

$$\mathcal{M} = \begin{pmatrix} \mathcal{C}_1^+ - \mathcal{C}_2^- & \mathcal{D}_2 & 0 & 0 & 0 \\ \mathcal{D}_2 & \mathcal{C}_2^+ - \mathcal{C}_3^- & \mathcal{D}_3 & 0 & 0 \\ 0 & \mathcal{D}_3 & \mathcal{C}_3^+ - \mathcal{C}_4^- & \ddots & 0 \\ \vdots & \vdots & \ddots & \ddots & \mathcal{D}_{N_V-1} \\ 0 & 0 & 0 & \mathcal{D}_{N_V-1} & \mathcal{C}_{N_V-1}^+ - \mathcal{C}_{N_V}^- \end{pmatrix} \quad \text{(C8)}$$

is an $(N_V - 1) \times (N_V - 1)$ tridiagonal matrix.

In the zero-pressure, $N_V = 3$ case, system (C3) is linear in $\{\Delta_l\}$ and the solution is

$$\Delta_1 = \frac{h_{13}}{1 + h_{13} + h_{23}} L_{sys}, \quad \text{(C9)}$$

$$\Delta_2 = \frac{h_{23}}{1 + h_{13} + h_{23}} L_{sys}, \quad \text{(C10)}$$

where

$$h_{13} \equiv \sqrt{(Q_1^2 + \hat{Q}_1^2)/(Q_3^2 + \hat{Q}_3^2)} \quad \text{(C11)}$$

and

$$h_{23} \equiv \sqrt{(Q_2^2 + \hat{Q}_2^2)/(Q_3^2 + \hat{Q}_3^2)} \quad \text{(C12)}$$

are given, and here we take $L_{sys} = 1$. The system (C7) can then be solved for $\mathbf{R}$ by inverting the matrix $\mathcal{M}$, namely, $\mathbf{R} = \mathcal{M}^{-1}\mathbf{S}$. Consider the limit defined in Sec. III, namely, $\iota_2^{\pm} = \pm X^{\alpha}$ and $\Delta\Psi_{t,2} = X^{\beta}$, where α, $\beta > 0$, and $X \to 0$. In this case, we have $\hat{Q}_2 = 0$, $Q_2 \sim X^{\beta}$, and $(Q_1, \hat{Q}_1, \bar{\mu}_1) = (Q_3, -\hat{Q}_3, \bar{\mu}_3) \equiv (Q, \hat{Q}, \bar{\mu})$, therefore $h_{13} = 1$ and $h_{23} \sim X^{\beta}$. Hence, as expected, $\lim_{X\to 0}\Delta_2 = 0$ and $\lim_{X\to 0}\Delta_1 = \lim_{X\to 0}\Delta_3 = 1/2$. On the other hand, all the elements of $\mathcal{M}$ go to zero in this limit, yet the elements of $\mathbf{S}$ do similarly and a non-trivial solution for $\mathbf{R}$ still exists. For $\alpha \geq \beta$, we get $\lim_{X\to 0} R_{1,1} = \kappa R_{0,1}$ and $\lim_{X\to 0} R_{2,1} = \kappa R_{3,1}$, which does not make the island vanish except in the trivial case $R_{0,1} = R_{3,1}$. For $\beta > \alpha$, however, we get

$$\lim_{X\to 0} R_{1,1} = \lim_{X\to 0} R_{2,1} = \frac{\kappa}{2}(R_{0,1} + R_{3,1}), \quad \text{(C13)}$$

and thus the island vanishes asymptotically as $X \to 0$. The function $\kappa \in [0, 1]$ is given by

$$\kappa = -\lim_{X\to 0}\frac{\mathcal{D}_3}{2\mathcal{C}_1^+} = \frac{k}{\bar{\mu}}\frac{\tan k + \cot k}{\tan\bar{\mu} + \cot\bar{\mu}}, \quad \text{(C14)}$$

where $k = \sqrt{\mu^2 - 1}/4$ and $\bar{\mu} = \mu/4$. Also, in the limit $X \to 0$, we have that $\iota_3^+ = \tan(\mu/2)$ and thus $\kappa = \kappa(\iota_3^+)$ only depends on the external rotational transform. Finally, one must be careful and verify that the two internal interfaces do not cross each other, i.e., check that $|R_{2,1} - R_{1,1}| < \Delta_2$ when the volume $\mathcal{V}_2$ is squeezed. For $\beta > \alpha$, we have $|R_{2,1} - R_{1,1}| \sim X^{\beta-\alpha}$ and therefore $|R_{2,1} - R_{1,1}|/\Delta_2 \sim X^{-\alpha}$. Thus, the only way to ensure that the two internal interfaces do never cross each other is to have $\alpha = 0$. Alternatively, one can first take the limit $\Delta\Psi_{t,2} \to 0$ and then take the limit $\iota_2^{\pm} \to 0$. In all cases, Eq. (C13) is satisfied.

[1]H. Grad, "Toroidal containment of a plasma," Phys. Fluids **10**(1), 137 (1967).
[2]J. R. Cary and M. Kotschenreuther, "Pressure induced islands in three-dimensional toroidal plasma," Phys. Fluids **28**(5), 1392 (1985).
[3]C. C. Hegna and A. Bhattacharjee, "Magnetic island formation in three-dimensional plasma equilibria," Phys. Fluids B **1**(2), 392 (1989).
[4]A. Bhattacharjee, T. Hayashi, C. C. Hegna, N. Nakajima, and T. Sato, "Theory of pressure-induced islands and self-healing in three-dimensional toroidal magnetohydrodynamic equilibria," Phys. Plasmas **2**(3), 883 (1995).
[5]P. Helander, "Theory of plasma confinement in non-axisymmetric magnetic fields," Rep. Prog. Phys. **77**(8), 087001 (2014).
[6]W. A. Newcomb, "Magnetic differential equations," Phys. Fluids **2**(4), 362 (1959).
[7]T. S. Hahm and R. M. Kulsrud, "Forced magnetic reconnection," Phys. Fluids **28**(8), 2412 (1985).
[8]M. N. Rosenbluth, R. Y. Dagazian, and P. H. Rutherford, "Nonlinear properties of the internal m = 1 kink instability in the cylindrical tokamak," Phys. Fluids **16**(11), 1894 (1973).
[9]W. Park, D. A. Monticello, R. B. White, and S. C. Jardin, "Non-linear saturation of the internal kink mode," Nucl. Fusion **20**(9), 1181–1185 (1980).
[10]C. Nuhrenberg and A. H. Boozer, "Magnetic islands and perturbed plasma equilibria," Phys. Plasmas **10**(7), 2840 (2003).
[11]J. Park, A. H. Boozer, and A. H. Glasser, "Computation of three-dimensional tokamak and spherical torus equilibria," Phys. Plasmas **14**(5), 052110 (2007).
[12]S. P. Hirshman, "Steepest-descent moment method for three-dimensional magnetohydrodynamic equilibria," Phys. Fluids **26**(12), 3553 (1983).
[13]J. B. Taylor, "Relaxation of toroidal plasma and generation of reverse magnetic fields," Phys. Rev. Lett. **33**(19), 1139–1141 (1974).
[14]M. D. Kruskal and R. M. Kulsrud, "Equilibrium of a magnetically confined plasma in a toroid," Phys. Fluids **1**(4), 265 (1958).
[15]H. K. Moffatt, "The degree of knottedness of tangled vortex lines," J. Fluid Mech. **35**(01), 117 (1969).
[16]M. A. Berger, "Introduction to magnetic helicity," Plasma Phys. Controlled Fusion **41**(12B), B167–B175 (1999).
[17]M. J. Hole, S. R. Hudson, and R. L. Dewar, "Equilibria and stability in partially relaxed plasma-vacuum systems," Nucl. Fusion **47**(8), 746–753 (2007).
[18]S. R. Hudson, M. J. Hole, and R. L. Dewar, "Eigenvalue problems for Beltrami fields arising in a three-dimensional toroidal magnetohydrodynamic equilibrium problem," Phys. Plasmas **14**(5), 052505 (2007).
[19]A. Bhattacharjee and R. L. Dewar, "Energy principle with global invariants," Phys. Fluids **25**(5), 887 (1982).
[20]G. R. Dennis, S. R. Hudson, R. L. Dewar, and M. J. Hole, "The infinite interface limit of multiple-region relaxed magnetohydrodynamics," Phys. Plasmas **20**(3), 032509 (2013).
[21]S. R. Hudson, R. L. Dewar, G. Dennis, M. J. Hole, M. McGann, G. von Nessi, and S. Lazerson, "Computation of multi-region relaxed magnetohydrodynamic equilibria," Phys. Plasmas **19**(11), 112502 (2012).
[22]M. McGann, S. R. Hudson, R. L. Dewar, and G. von Nessi, "Hamilton-Jacobi theory for continuation of magnetic field across a toroidal surface

supporting a plasma pressure discontinuity," Phys. Lett. A **374**(33), 3308–3314 (2010).
[23]J. D. Meiss, "Symplectic maps, variational principles, and transport," Rev. Mod. Phys. **64**(3), 795–848 (1992).
[24]R. L. Dewar, A. Bhattacharjee, R. M. Kulsrud, and A. M. Wright, "Plasmoid solutions of the Hahm-Kulsrud-Taylor equilibrium model," Phys. Plasmas **20**(8), 082103 (2013).
[25]P. R. Garabedian, *Magnetohydrodynamic Stability of Fusion Plasmas* (John Wiley and Sons, 1998), Vol. LI, pp. 1019–1033.
[26]G. R. Dennis, S. R. Hudson, D. Terranova, P. Franz, R. L. Dewar, and M. J. Hole, "Minimally constrained model of self-organized helical states in reversed-field pinches," Phys. Rev. Lett. **111**(5), 055003 (2013).
[27]F. L. Waelbroeck, "Current sheets and nonlinear growth of the $m = 1$ kink-tearing mode," Phys. Fluids B **1**(12), 2372 (1989).
[28]A. H. Boozer and N. Pomphrey, "Current density and plasma displacement near perturbed rational surfaces," Phys. Plasmas **17**(11), 110707 (2010).
[29]R. B. White, "Representation of ideal magnetohydrodynamic modes," Phys. Plasmas **20**(2), 022105 (2013).